Polymer Self-Assembly

DOI: 10.1002/anie.201102280

Molecular Self-Assembly of a Homopolymer: An Alternative To Fabricate Drug-Delivery Platforms for Cancer Therapy**

Jinyao Liu, Wei Huang, Yan Pang, Ping Huang, Xinyuan Zhu, Yongfeng Zhou, and Deyue Yan**

Molecular self-assembly of synthetic polymers in a selective solvent or through layer-by-layer approaches has attracted great interest.[1,2] Most reported precursors for the self-assembly in selective solvents are amphiphilic linear/dendritic block copolymers.[3,4] Recently, the covalent block precursors have been extended to supramolecular ones.[5] However, little attention has been paid to the molecular self-assembly of a homopolymer derived from only one type monomer. Is there any homopolymer that can spontaneously aggregate into highly ordered structures driven by noncovalent interactions? To answer this question, we synthesized a novel amphiphilic homopolymer and realized its aqueous self-assembly to form spherical micelles with a remarkably narrow size distribution. The resulting micelles exhibit smart redox-responsive properties, which can be exploited to rapidly deliver hydrophobic drugs into the nuclei of tumor cells and enhance the inhibition of cell proliferation.

The monomer used is 2-[(2-hydroxyethyl)-disulfanyl]ethoxy-2-oxo-1,3,2-dioxaphospholane, which consists of both hydrophobic and hydrophilic moieties and can polymerize into a hyperbranched polyphosphate (HPHDP) through self-condensing ring-opening polymerization (SCROP).[6] HPHDP is an amphiphilic homopolymer with alternative hydrophobic disulfide and hydrophilic polyphosphate segments along the highly branched structure (Scheme 1). Three HPHDP samples with different molecular weights were synthesized. Characterization data of the different precursor samples and corresponding micelles are summarized in Table 1.[7] In general, the molecular-weight distribution of a hyperbranched polymer is very broad. However, the low-molecular-weight species in the products were removed by dialysis, so the M_w/M_n value of the final samples is equal to or less than 1.72. The degrees of branching (DBs) measured by NMR spectroscopy approach 0.5. Figure 1a shows a typical transmission electron microscopy (TEM) image of HPHDP micelles, and Figure 1b is the enlarged TEM image of only one micelle. It is interesting that the micelles are fairly homogeneous. Statistical analyses based on 100 micelles for each HPHDP sample (Figure 1c)

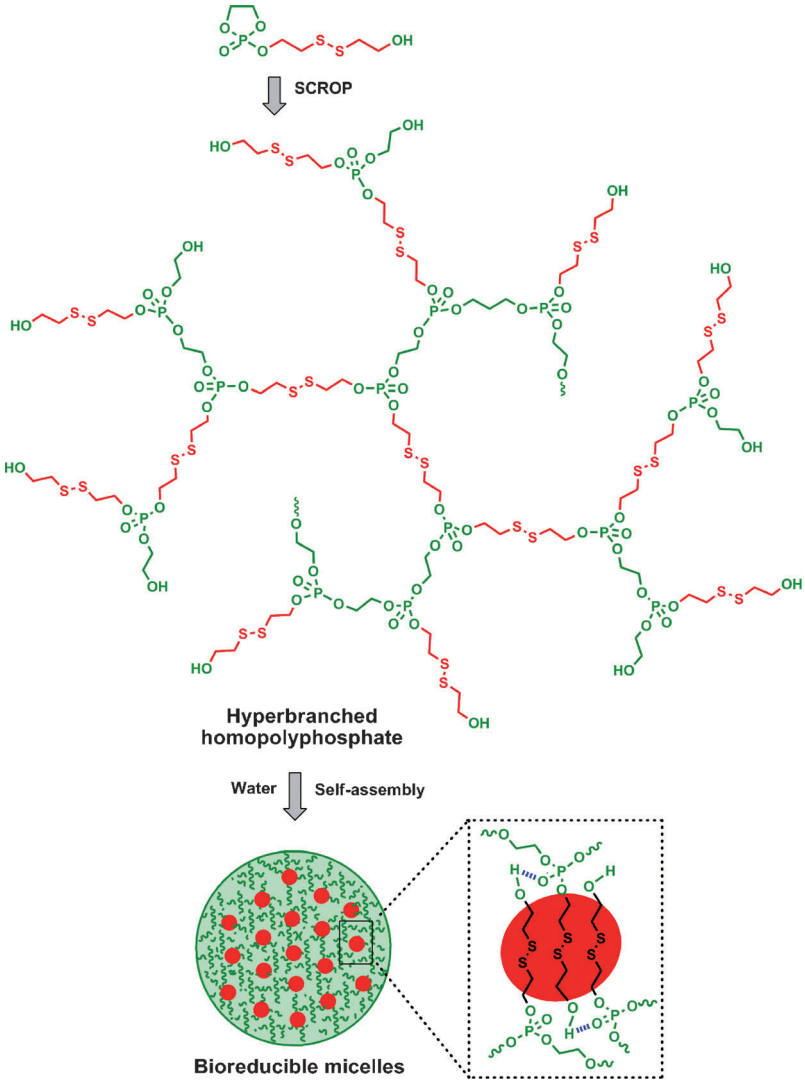

Scheme 1. Synthesis of HPHDP and schematic representation of the self-assembled micelles.

[*] J. Y. Liu, Prof. Dr. W. Huang, Y. Pang, P. Huang, Prof. Dr. X. Y. Zhu, Prof. Dr. Y. F. Zhou, Prof. Dr. D. Y. Yan
School of Chemistry and Chemical Engineering
Shanghai Jiao Tong University
State Key Laboratory of Metal Matrix Composites
800 Dongchuan Road, Shanghai, 200240 (P. R. China)
E-mail: hw66@sjtu.edu.cn
dyyan@sjtu.edu.cn

[**] Financial support was provided by the National Basic Research Program (2007CB808000, 2009CB930400), National Natural Science Foundation of China (No. 21074069, 20874060, 50873058).

Supporting information for this article is available on the WWW under http://dx.doi.org/10.1002/anie.201102280.

Table 1: Details of HPHDP and its self-assembled micelles.[a]

Sample	M_n [g mol^{-1}]	M_w [g mol^{-1}]	M_w/M_n	DB	D [nm]	PDI
$HPHDP_1$	11210	19290	1.72	0.47	78	0.07
$HPHDP_2$	6560	9970	1.52	0.48	53	0.12
$HPHDP_3$	3140	4060	1.29	0.50	30	0.17

[a] M_n = Number-average molecular weight, M_w = weight-average molecular weight, DB = degree of branching, D = diameter of micelles, PDI = polydispersity index of micelles determined by DLS.

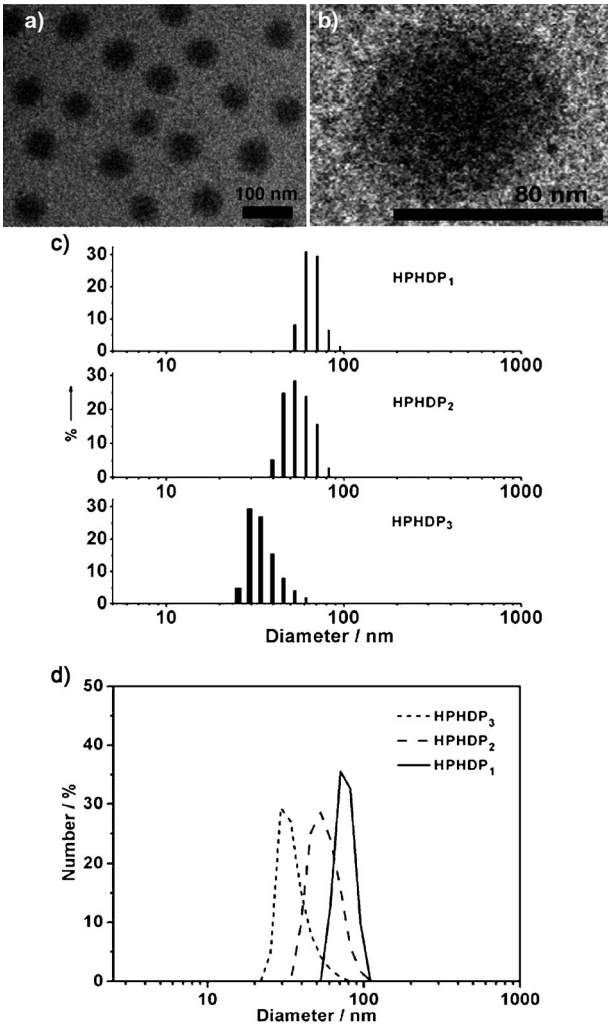

Figure 1. Representative TEM images of a) narrow-size-distribution $HPHDP_1$ micelles and b) the unique multi-core/shell aggregating structure. c) Size distributions of HPHDP micelles based on a statistical evaluation. d) DLS curves of HPHDP micelle solutions with concentration 1.0 mg mL^{-1}.

further demonstrate the narrow size distribution of the micelles. The dynamic light scattering (DLS) curves (Figure 1d) are in agreement with the statistical diagrams. The average diameter of HPHDP micelles is highly dependent on the molecular weight and increases from 30 to 78 nm when the number-average molecular weight is increased from 3140 to 11210 g mol^{-1} (Table 1). The dependence of the micelle size on molecular weight is similar to that of the linear block copolymer micelles.[1d]

The micellization process was characterized by fluorescence technique with pyrene as a probe. I_1 and I_3 are the emission intensity of the first and third bands in the fluorescence spectrum of pyrene, respectively (labeled 1 and 3 in the inset of Figure 2a). The ratio of I_3/I_1 is very sensitive to the polarity of the medium surrounding pyrene molecules.[8] As shown in Figure 2a, the I_3/I_1 values remain nearly unchanged at low concentrations of HPHDP, thus indicating the characteristics of pyrene molecules in aqueous environment. With increasing concentration of HPHDP, the I_3/I_1 value starts to increase dramatically and reaches a level typical of pyrene molecules in a completely hydrophobic environment, thus implying the formation of hydrophobic microdomains within the micelles and the micellization of HPHDP. The micelle formation was also validated by measuring the surface tension of HPHDP aqueous solution at various HPHDP concentrations. The plot of surface tension versus the logarithm of HPHDP concentration ($\log c$) shows that the limiting surface tension is 63.3 mN m^{-1} and a break occurs at 1.0×10^{-3} g L^{-1} (Figure 2b), which also indicates the micellization process.[9] Besides, the variable-temperature Fourier transform infrared spectrometer (FTIR) was adopted to characterize the existence of H-bonds in HPHDP micelles (Figure 2c). With the temperature increasing from 20 to 180 °C, the broad peak in the range of 3030–3750 cm^{-1} belong to the hydroxy groups gradually becomes narrower and a small blue shift occurs. Meanwhile, the peak at 1645 cm^{-1} assigned to the H-bonding P=O groups disappeared. These data convincingly suggest the existence of the H-bonds within HPHDP micelles, and they are destroyed with increasing temperature. So, we can conclude that the micellization process is driven by the inter- and intramolecular interactions, including the microphase separation of hydrophobic $CH_2CH_2SSCH_2CH_2$ segments as well as the H-bonds between OH and P=O groups.

We attributed the special assembly ability of HPHDP to the unique molecular structure. Since the DBs of HPHDP samples are approximately 0.5, almost half of the hydrophobic disulfide segments are terminal. In addition, the backbone of HPHDP is very flexible, which can easily accommodate the conformational change during phase segregation. Therefore, both intra- and intermolecular microphase segregation may occur rapidly. The mutual repulsion stemming from the immiscibility of the two types of segments drives the system to segregate and induces the microphase separation in the selective solvent, thus forming a core/shell structure. Owing to the limited sizes of the large number of hydrophobic and hydrophilic segments in the precursor molecules, it seems impossible to form a micelle of several tens nanometers with only one hydrophobic core. The enlarged TEM image (Figure 1b) clearly shows that the micelle is composed of a lot of small black domains (attributed to the aggregated hydrophobic disulfide segments), and the hydrophobic microdomains are surrounded by the continuous hydrophilic phase (attributed to the aggregated polyphosphate segments). The directional H-

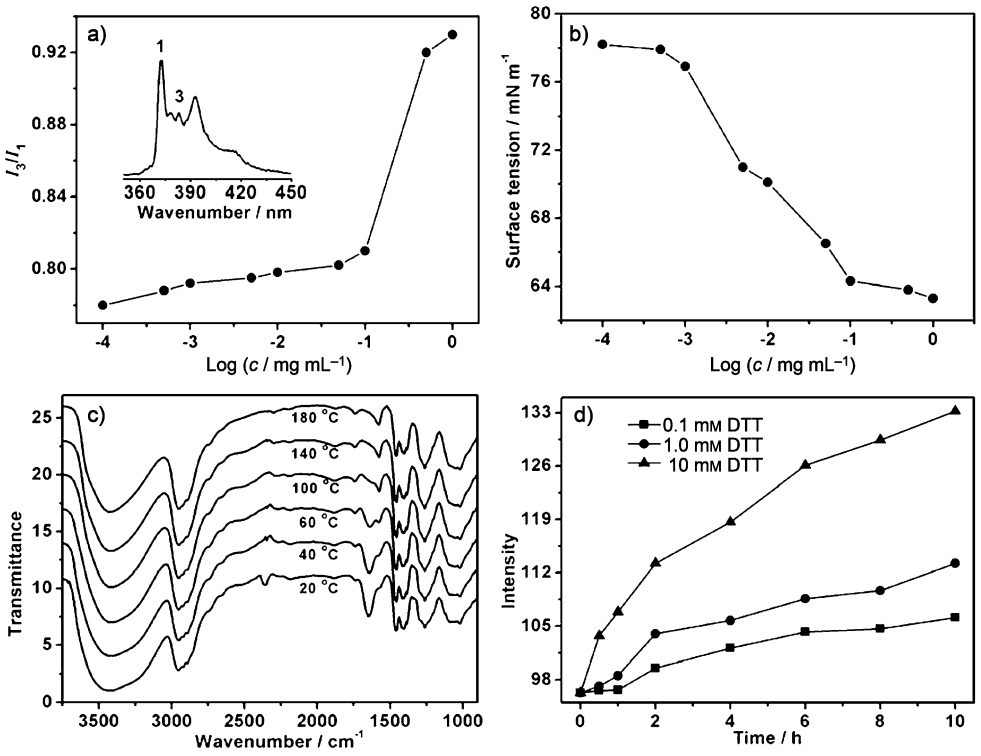

Figure 2. a) Relationship between the fluorescence intensity ratio (I_3/I_1) and $HPHDP_1$ concentration in aqueous solution (Inset: fluorescence emission spectrum of pyrene). b) The relationship of surface tension and concentration of $HPHDP_1$ aqueous solution. c) Variable-temperature FTIR spectra of dried $HPHDP_1$ micelles. d) DOX released from $HPHDP_1$ micelles by treatment with DTT at various concentrations, as monitored by the fluorescence intensity of DOX (554 nm).

bonds stabilized the aggregation of HPHDP. So a multi-core/shell structure of the micelle is supposed (Scheme 1). The micellization process includes the segregation of hydrophobic and hydrophilic segments and the aggregation of HPHDP molecules. Both the segregation and the aggregation occurred simultaneously. This process is a dynamic one, and the dynamics are more prominent for the aggregation of HPHDP with lower molecular weight, which leads to a broader size distribution (Table 1). In other words, the higher the molecular weight of HPHDP, the narrower the size distribution of the resulting micelles.

The redox-responsive properties of HPHDP micelles under reductive environments has been tested by measuring the fluorescence intensity of doxorubicin (DOX)-loaded HPHDP micelles in phosphate-buffered saline (PBS) after treatment with DL-1,4-dithiothreitol (DTT) as demonstrated in Figure 2d. Faster DOX release is observed with increasing DTT concentration. It has been reported that incorporation of DOX into the hydrophobic core of micelles decreases the fluorescence intensity of DOX relative to free DOX at the same concentration.[10] Therefore, the enhanced fluorescence should be attributed to the rapid DOX release from the micelles.

We are interested in the redox-responsive properties of HPHDP micelles in living cells. It is well documented that glutathione monoester (GSH-OEt) can penetrate cellular membranes and rapidly reach a high intracellular concentration of glutathione (GSH).[11] As a model system, Hela cells (a human cervical carcinoma cell line) were first incubated with 10 mM GSH-OEt for 2 h to manipulate the intracellular concentration of GSH and then incubated with DOX-loaded HPHDP micelles. Hela cells that had not been pretreated with GSH-OEt were used as control. Confocal laser scanning microscopy (CLSM) images show that the intracellular DOX fluorescence in the GSH-OEt pretreated cells is mainly located at the nucleus (Figure 3a) compared to the control cells (Figure 3b), which indicates the rapid release and nucleus localization of DOX in cells. These results were further confirmed by flow cytometric analyses. As given in Figure 3c, the DOX fluorescence intensity of all pretreated cells is higher than that of control cells. Obviously, the pretreatment of Hela cells with GSH-OEt can up-regulate the intracellular concentration of GSH, accelerate the degradation of disulfide bonds, and rapidly release DOX from HPHDP micelles intracellularly.

The inhibition of tumor cell proliferation in vitro of DOX-loaded HPHDP micelles was also studied. It is well known that buthionine sulfoximine (BSO) is an inhibitor for the intracellular synthesis of GSH.[12] Here Hela cells were treated with 10 mM GSH-OEt for 2 h and 0.1 mM BSO for 12 h respectively, then incubated with the DOX-loaded micelles. Simultaneously, the non-pretreated cells were used as control. As shown in Figure 3d, the 50% cellular growth inhibition (IC_{50}) values of the control, the GSH-OEt pretreated cells, and the BSO pretreated Hela cells are 0.35, 0.08, and 0.64 $\mu g\,mL^{-1}$, respectively. By comparison of above results, the Hela cells pretreated by GSH-OEt and BSO exhibit enhanced and decreased inhibition efficiencies, respectively. The decreased efficiency may be attributed to the presence of BSO, which reduced the intracellular concentration of GSH, suppressed the disaggregation of DOX-loaded micelles, and finally decreased the DOX release. These results well demonstrate the redox-responsiveness of HPHDP micelles. In other words, the rapid destabilization of the micelles triggered by higher intracellular concentration of GSH leads to accelerated DOX release and enhanced inhibition of cell proliferation.

In summary, an amphiphilic hyperbranched homopolymer with alternating hydrophobic disulfide and hydrophilic polyphosphate segments along the highly branched structure was synthesized by SCROP of the monomer consisting of both

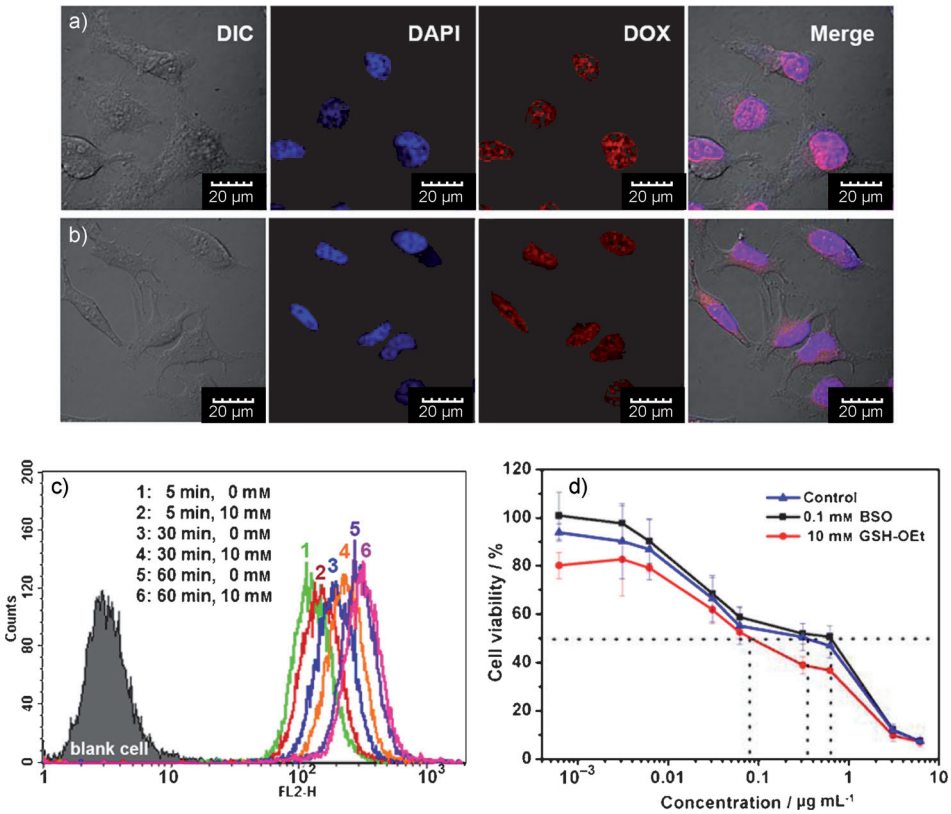

Figure 3. a) Representative CLSM images of Hela cells incubated with DOX-loaded $HPHDP_1$ micelles for 1 h a) with or b) without pretreatment with 10 mM GSH-OEt for 2 h (cell nuclei were stained with DAPI = 2-(4-amidinophenyl)-6-indolecarbamidine dihydrochloride). DIC = differential interface contrast. c) Flow cytometric histogram profiles of Hela cells incubated with DOX-loaded $HPHDP_1$ micelles for different time intervals. The cells were either not pretreated or pretreated with 10 mM GSH-OEt. FL2-H = fluorescence intensity of DOX. d) Viability of Hela cells cultured with DOX-loaded $HPHDP_1$ micelles at different drug concentrations for 48 h. The cells were pretreated with 10 mM GSH-OEt or 0.1 mM BSO. The non-pretreated cells were used as control. Data are presented as the average ± standard deviation ($n = 6$).

hydrophobic and hydrophilic moieties. This homopolymer is a novel precursor for molecular self-assembly. The resulting micelles possess a multi-core/shell structure and a narrow size distribution. Furthermore, the micelles are stable in aqueous solution, while they exhibit smart response in a reductive environment. With the help of HPHDP micelles, hydrophobic anticancer drugs could be rapidly and efficiently transported into the nuclei of tumor cells and show enhanced inhibition of cell proliferation. Therefore, the self-assembly of homopolymers extends the field of molecular self-assembly and provides a favorable platform to construct excellent drug-delivery systems for cancer therapy.

Received: April 1, 2011
Revised: June 17, 2011
Published online: August 24, 2011

Keywords: antitumor agents · drug delivery · polymers · redox chemistry · self-assembly

[1] a) L. Zhang, A. Eisenberg, *Science* **1995**, *268*, 1728; b) L. Zhang, K. Yu, A. Eisenberg, *Science* **1996**, *272*, 1777; c) D. E. Discher, A. Eisenberg, *Science* **2002**, *297*, 967; d) L. Zhang, A. Eisenberg, *Polym. Adv. Technol.* **1998**, *9*, 677.

[2] a) M. Haubs, H. Ringsdorf, *Angew. Chem.* **1985**, *97*, 880; *Angew. Chem. Int. Ed.* **1985**, *24*, 882; b) H. Ringsdorf, B. Schlarb, J. Venzmer, *Angew. Chem.* **1988**, *100*, 117; *Angew. Chem. Int. Ed.* **1988**, *27*, 113.

[3] a) Y.-Y. Won, H. T. Davis, F. S. Bates, *Science* **1999**, *283*, 960; b) S. Jain, F. Bates, *Science* **2003**, *300*, 460; c) X. Wang, G. Guerin, H. Wang, Y. Wang, I. Manners, M. A. Winnik, *Science* **2007**, *317*, 644; d) H. Cui, Z. Chen, S. Zhong, K. L. Wooley, D. J. Pochan, *Science* **2007**, *317*, 647; e) B. M. Dische, Y. Y. Won, D. S. Ege, J. C. Lee, F. S. Bates, D. E. Discher, D. A. Hammer, *Science* **1999**, *284*, 1143; f) S. A. Jenekhe, X. L. Chen, *Science* **1998**, *279*, 1903; g) S. I. Stupp, V. LeBonheur, K. Walker, L. S. Li, K. E. Huggins, M. Keser, A. Amstutz, *Science* **1997**, *276*, 384; h) J. D. Hartgerink, E. Beniash, S. I. Stupp, *Science* **2001**, *294*, 1684; i) T. Kato, *Science* **2002**, *295*, 2414; j) G. M. Whitesides, M. Boncheva, *Proc. Natl. Acad. Sci. USA* **2002**, *99*, 4769.

[4] a) J. C. M. Van Hest, D. A. P. Delnoye, M. W. P. L. Baars, M. H. P. van Genderen, E. W. Meijer, *Science* **1995**, *268*, 1592; b) S. Peleshanko, V. V. Tsukruk, *Prog. Polym. Sci.* **2008**, *33*, 523; c) Y. F. Zhou, D. Y. Yan, *Chem. Commun.* **2009**, 1172; d) A. P. H. J. Schenning, C. Elissen-Román, J.-W. Weener, M. W. P. L. Baars, S. J. van der Gaast, E. W. Meijer, *J. Am. Chem. Soc.* **1998**, *120*, 8199; e) M. Ornatska, S. Peleshanko, K. L. Genson, B. Rybak, K. N. Bergman, V. V. Tsukruk, *J. Am. Chem. Soc.* **2004**, *126*, 9675; f) M. Ornatska, K. N. Bergman, B. Rybak, S. Peleshanko, V. V. Tsukruk, *Angew. Chem.* **2004**, *116*, 5358; *Angew. Chem. Int. Ed.* **2004**, *43*, 5246; g) M. Ornatska, S. Peleshanko, B. Rybak, J. Holzmueller, V. V. Tsukruk, *Adv. Mater.* **2004**, *16*, 2206; h) D. Y. Yan, Y. F. Zhou, J. Hou, *Science* **2004**, *303*, 65; i) M. Calderón, M. A. Quadir, S. K. Sharma, R. Haag, *Adv. Mater.* **2010**, *22*, 190; j) Y. F. Zhou, W. Huang, J. Y. Liu, X. Y. Zhu, D. Y. Yan, *Adv. Mater.* **2010**, *22*, 4567.

[5] a) L. Brunsveld, B. J. B. Folmer, E. W. Meijer, R. P. Sijbesma, *Chem. Rev.* **2001**, *101*, 4071; b) D. Y. Chen, M. Jiang, *Acc. Chem. Res.* **2005**, *38*, 494; c) C. Fouquey, J.-M. Lehn, A. M. Levelut, *Adv. Mater.* **1990**, *2*, 254; d) R. P. Sijbesma, F. H. Beijer, L. Brunsveld, B. J. B. Folmer, J. H. K. K. Hirschberg, R. F. M. Lange, J. K. L. Lowe, E. W. Meijer, *Science* **1997**, *278*, 1601; e) J. H. K. K. Hirschberg, L. Brunsveld, A. Ramzi, J. A. J. M. Vekemans, R. P. Sijbesma, E. W. Meijer, *Nature* **2000**, *407*, 167; f) X. Zhang, C. Wang, *Chem. Soc. Rev.* **2011**, *40*, 94.

[6] a) J. Y. Liu, W. Huang, Y. F. Zhou, D. Y. Yan, *Macromolecules* **2009**, *42*, 4394; b) J. Y. Liu, Y. Pang, W. Huang, X. Zhai, X. Y. Zhu, Y. F. Zhou, D. Y. Yan, *Macromolecules* **2010**, *43*, 8416.

[7] See the Supporting Information for details.
[8] a) G. Kwon, M. Naito, M. Yokoyama, T. Okano, Y. Sakurai, K. Kataoka, *Langmuir* **1993**, *9*, 945; b) J. Rodriguez-Hernandez, F. Checot, Y. Gnanou, S. Lecommandoux, *Prog. Polym. Sci.* **2005**, *30*, 691.
[9] P. H. Ni, M. Z. Zhang, L. H. Ma, S. K. Fu, *Langmuir* **2006**, *22*, 6016.
[10] a) M. Oishi, H. Hayashi, I. D. Michihiro, Y. Nagasaki, *J. Mater. Chem.* **2007**, *17*, 3720; b) Y. Bae, S. Fukushima, A. Harada, K. Kataoka, *Angew. Chem.* **2003**, *115*, 4788; *Angew. Chem. Int. Ed.* **2003**, *42*, 4640.
[11] a) A. N. Koo, H. J. Lee, S. E. Kim, J. H. Chang, C. Park, C. Kim, J. H. Park, S. C. Lee, *Chem. Commun.* **2008**, 6570; b) R. Hong, G. Han, J. M. Fernandez, B. J. Kim, N. S. Forbes, V. M. Rotello, *J. Am. Chem. Soc.* **2006**, *128*, 1078.
[12] J. E. Liebmann, S. M. Hahn, J. A. Cook, C. Lipschultz, J. B. Mitchell, D. C. Kaufman, *Cancer Res.* **1993**, *53*, 2066.

